



## Dynamics of the long-period tides

CARL WUNSCH<sup>1</sup>, DALE B. HAIDVOGEL<sup>2</sup>, MOHAMED ISKANDARANI<sup>2</sup> and R. HUGHES<sup>3</sup>

<sup>1</sup>*Department of Earth, Atmospheric and Planetary Sciences, Massachusetts Institute of Technology, Cambridge, MA 02139, USA*

<sup>2</sup>*Institute of Marine and Coastal Sciences, Rutgers University, New Brunswick, NJ 08903, USA*

<sup>3</sup>*625 Ross River Road, Kirwan, Qld 4817, Australia*

**Abstract** – The long-period tides are a tool for understanding oceanic motions at low frequencies and large scales. Here we review observations and theory of the fortnightly, monthly and pole tide constituents. Observations have been plagued by low signal-to-noise ratios and theory by the complex lateral geometry and great sensitivity to bottom slopes. A new spectral element model is used to compute the oceanic response to tidal forcing at 2-week and monthly periods. The general response is that of a heavily damped ( $Q \approx 5$ ) system with both the energy input from the moon and the dissipation strongly localized in space. The high dissipation result is probably generally applicable to all low frequency barotropic oceanic motions. Over much of the ocean, the response has both the character of a large-scale and a superposed Rossby wave-like character, thus vindicating two apparently conflicting earlier interpretations. To the extent that free waves are excited they are consistent with their being dominated by Rossby and topographic Rossby wave components, although gravity modes are also necessarily excited to some degree. In general, a modal representation is not very helpful. The most active regions are the Southern Ocean and the western and northern North Atlantic. These results are stable to changes in geometry, topography, and tide period. On a global average basis, the dynamical response of Mm is closer to equilibrium than is Mf. © 1998 Elsevier Science Ltd. All rights reserved

### 1. INTRODUCTION

The long-period tides at 8 days, 2 weeks, 1 month, 6 months, ..., 18.6 years, etc., have been studied since the time of Laplace. WUNSCH (1967) reviewed the considerable late nineteenth and early twentieth century analytical work by Kelvin, Rayleigh, Poincaré, Proudman, and others. From the point of view of modern oceanography, one is interested in these phenomena for the light they may shed on the more general motions existing in the ocean at low frequencies; some general background can be found in HENDERSHOTT (1981) and a general historical treatment can be found in CARTWRIGHT (1998). They are also of concern in studies of the rotation of the earth and are now a significant contributor to sea level variations as seen by the latest altimetric missions.

Studies of wind- and/or buoyancy-driven motions in the ocean at long periods are made complicated by the considerable remaining uncertainties in the structure of the forcing functions (uncertainties in the wind stress, etc.), which render highly ambiguous many inferences about the oceanic response. In contrast, the periods and structures of the long-period tides are known with literal astronomical precision, and no ambiguity deriving from their uncertainty propagates through the observations or theory. But the price one pays for studying these tides is not small:

the motions are relatively weak; they are curl free; the forcing has no longitude dependence; and they are narrow-band deterministic forces whose response usually carries less information than does that from broadband stochastic driving.

After examining the available tide gauge records from islands in the tropical and sub-tropical Pacific (typically 4 years in duration at most), WUNSCH (1967) suggested that the oceanic response to long-period tide forcing would be dominated by the generation at the lateral boundaries of barotropic Rossby waves. He offered a crude solution for a rectangular  $\beta$ -plane ocean of roughly Pacific Ocean dimensions, in which the oceanic response was equilibrium plus a sum over the Rossby wave modes of the box. Apparent small spatial scales in the tide gauge results were to be explained by the presence of the waves.

In the 30 years since then, there has been a small number of papers published on the long-period tides, including KAGAN, RIVKIND and CHERNAYEV (1976), LUTHER (1980), CARTON (1983), O'CONNOR (1995), SCHWIDERSKI (1982), DICKMAN (1989), SEILER (1990), RAY and CARTWRIGHT (1994) and a few others. MILLER, LUTHER and HENDERSHOTT (1993) review much of this literature. A small separate literature on the 14-month pole tide, which is not of gravitational origin and for which the forcing does have a longitudinal dependence, will be considered separately below. We are motivated to re-open the question of the nature of the oceanic response to long-period tide forcing for a number of reasons. (1) The now 4-year long TOPEX/POSEIDON altimeter record should soon become adequate to produce high accuracy, truly global estimates of the fortnightly and monthly tides. (2) Numerical models have advanced to the stage where calculations of the tidal response are "almost easy". (3) MILLER *et al.* (1993), using a numerical model, drew the very surprising conclusion that in the Pacific Ocean at least, the dominant response was not primarily a Rossby wave, but was produced by a Kelvin wave response propagating from a generation region in the Arctic Ocean. If their conclusion is correct, it needs rationalization and much better understanding. (4) Finally, and probably most important, issues of oceanic dissipation remain vexingly obscure; the response of long period tides may well represent the most direct path to understanding the oceanic dissipation of barotropic motions generally.

Our focus here is on understanding the physics of the response to potential forces acting on the ocean at long periods with a numerical model as our primary tool. It is specifically not our intention to model the altimeter results in detail—a job that others are undertaking. Consequently, we omit such important (but not fundamental) details as a treatment of tidal self-attraction and load tides, and indeed have felt free to change the forcing frequencies to suit our convenience. The extraction of the Mf and Mm constituents from TOPEX/POSEIDON data is still not definitive; but within about 2 years, there should be quite dramatic improvements in the description of the detailed structure of the oceanic response. Thus the time seems ripe to undertake an overview of this subject.

## 2. EQUATIONS AND THE MODEL

The gravitational long-period tides (what Laplace called "tidal species 1"—see LAMB, 1932) are all of equilibrium form

$$\bar{\eta} = H(\sigma)Y_2^0(\cos \theta)\exp(-i\sigma t) \quad (1)$$

where  $Y_2^0$  is the spherical harmonic of degree 2 and order 0, and  $\theta$  is the co-latitude.  $\sigma$  is the

tidal frequency corresponding to 2 weeks (the strongest long-period tide), 8 days, 1 month, etc.  $H(\sigma)$  is an amplitude. There is no longitude,  $\lambda$ , dependence in (1). Standard references for the amplitudes are DOODSON (1921), SCHUREMAN (1958) or CARTWRIGHT and EDDEN (1973). Under the (good) assumption of linear dynamics, the governing equations are the Laplace Tidal Equations (LTE) on the sphere with real topography. These equations are not reproduced here but may be found in LAMB (1932), LONGUET-HIGGINS (1968), GILL (1982) or in many other books and papers. To be specific, we will focus here on the fortnightly tide Mf whose period is 327.86 h (13.66 days), but will also touch on the monthly Mm constituent (period 661.31 h, 27.6 days). The major solar contributions at 6 months ( $S_{sa}$ ) and annual ( $S_a$ ) are dominated by thermal effects, and thus their gravitational component will be treated here only implicitly.

The important features of the forcing function in Eq. (1) are that  $\bar{\eta}$  is curl free, and that it is a function of latitude (or co-latitude) alone. WUNSCH (1967) discusses the many attempts to solve the LTE at low frequencies on a water-covered globe. The physical argument is simple and worth recalling. At a period of 2 weeks, and away from the immediate vicinity of the equator, one anticipates any oceanic dynamical response to be nearly geostrophic. If the ocean floor were uniform,  $\bar{\eta}$  would set up a quasi-geostrophic flow field, dominated by flow in the zonal direction, and which would simply oscillate with frequency  $\sigma$ . If the sea surface elevation is  $\eta$ , the magnitude of the flow would be nearly,

$$u = \frac{g}{f(\theta)} \frac{\partial(\eta - \bar{\eta})}{a\partial\theta}, \quad |v| = O\left(\frac{\sigma}{f} |u|\right) \quad (2)$$

because  $\sigma \ll f$ , where, conventionally,  $g$  is gravity,  $f$  is the Coriolis parameter,  $\theta$  is co-latitude, and  $a$  is the mean earth radius. (Eq. (2) is invalid very near the equator.) Higher order dynamics, including dissipation, determine the extent to which  $\eta$  differs from  $\bar{\eta}$ . If  $\eta = \bar{\eta}$ , one has the so-called "equilibrium tide" and the small horizontal flow exists only to provide the slight necessary divergence. These solutions are straightforward and are discussed at length in the references, including cases in which the bottom depth is a function of  $\theta$  alone.

Difficulties arise as soon as the zonal flow is blocked by a continental boundary or by a seafloor ridge system. It was WUNSCH's (1967) conclusion that the boundary condition of no normal flow, or at any feature capable of supporting a zonal pressure gradient, would be satisfied by the generation of barotropic Rossby waves able to produce a zonal velocity zero at a wall, or to match a mass-flux condition at a depth change.

For a general bounded ocean basin, the solution can be written

$$\eta = \bar{\eta} + \frac{1}{h} \sum_n \sum_m a_{nm} \cdot (\text{normal mode})_{nm} \quad (3)$$

The factor  $1/h$  has been separated from the  $a_{nm}$ , to emphasize that as  $h \rightarrow \infty$  all tides tend to approach equilibrium in the absence of true resonance. One may summarize much of the literature of the last 30 years as questioning the extent to which large spatial-scale normal modes are significant in the sense that a few of the terms in Eq. (3) are relatively strongly excited in a near-resonance, as WUNSCH (1967) supposed, or many modes are more or less all weakly excited as, for example, LUTHER (1980) concluded.

Double indices  $n, m$  have been used in Eq. (3) because for a bounded two-dimensional ocean, one anticipates a two-parameter family set of eigenfunctions of the Laplace Tidal Equations.

LONGUET-HIGGINS and POND (1970) computed the normal modes of a flat-bottomed hemispherical ocean, and PLATZMAN, CURTIS, HANSEN and SLATER (1981) computed them for a realistic ocean with bottom topography. Even for the flat-bottomed hemisphere, the modes are not simple, but in various degrees of approximation can be divided into gravity and Rossby wave modes. When real topography is introduced, the Rossby waves are broken up into topographic Rossby waves, often tightly confined geographically to specific bottom features (see PLATZMAN *et al.*, 1981). Physically, however, the gravity wave branch at high frequencies and the Rossby wave/topographic Rossby wave branch at low frequencies persist as recognizable phenomena in all these solutions. A mode deriving directly from the Kelvin wave, as always, remains an exceptional solution existing at both low and high frequencies. Its low frequency cut-off is dictated by the wavelength exceeding the earth's circumference. All this discussion is quite loose, as the meaning of a Kelvin wave having a barotropic deformation radius,  $\sqrt{gh}/f$ , of several thousand kilometers is not always clear, but some of the modes clearly possess Kelvin-wave like behavior. (O'CONNOR, 1995, has confused the issue by labelling the Rossby wave modes as "inertia gravity waves"—a clear misnomer.)

For a linear system, the representation (3) is exact and to the extent that the normal modes are known, a formal solution to the LTE can always be found. The interesting question lies with the interpretation of the modes: whether some amplitudes are much larger than others, and whether those particular modes are readily interpreted in simple form as Rossby waves, Kelvin waves, etc. It is important to recognize that in a globally forced problem like this one, the modal amplitudes in a representation such as in Eq. (3) are not unique. The solution can also be written as

$$\eta = (\text{particular solution}) + (\text{homogeneous solution}) \quad (4)$$

where the homogeneous solution is a different sum of normal modes than in Eq. (3). Because we are free to choose a particular solution in infinitely many ways, the amplitudes of these normal modes will change correspondingly in an infinite number of ways. A normal mode expansion of the sum in Eqs (3) or (4) is, however, unique.

Amplitudes of normal modes in a dissipationless system will occur in the general (and abstract) form

$$a_{nm} = \frac{F_{nm}(\text{geometry})}{l(\sigma)^2 - q(n,m)^2} \quad (5)$$

that is with an order one factor,  $F_{nm}$ , depending upon the geometry, and an overall amplitude dependent upon whether the denominator is close to zero or not.  $l$  is a wavenumber representing the forcing function. A vanishing denominator corresponds to a resonant mode at frequency  $\sigma$ .  $q(n,m)$  is in general a transformation from the indices  $n, m$  to corresponding horizontal wavenumbers (a specific case is shown in WUNSCH, 1967, Eq. 29). The presence of dissipation usually renders  $l(\sigma)^2$  complex, so that no true infinity can occur.

Formally, one can expect that all possible modes are excited to some degree, as long as the projection of the modes onto the forcing, implicit in  $F_{nm}$ , does not vanish. In particular, MILLER *et al.* (1993) interpret their solution as showing the major excitation of the gravity wave modes in addition to the Rossby modes. Simple interpretation is possible, however, only if a small number of modes dominates the response. If many spatially complicated modes are present

and/or they are heavily dissipated, the normal mode representation—although remaining mathematically valid—may no longer be an enlightening framework.

For insight into the problem, we will avoid the use of normal modes and solve the forced problem directly with the spectral element ocean model (SEOM) of ISKANDARANI, HAIDVOGEL and BOYD (1995) and HAIDVOGEL, CURCHITSER, ISKANDARANI, HUGHES and TAYLOR (1997). Although such models are novel in oceanography, they have been widely used in other branches of fluid dynamics and we anticipate a more accurate solution than can be obtained with more conventional representations.

SEOM solves the shallow water equations:

$$\mathbf{u}_t + \mathbf{u} \cdot \nabla \mathbf{u} + \mathbf{f} \times \mathbf{u} = -g \nabla(\eta - \bar{\eta}) - \frac{r\mathbf{u}}{h} + \frac{\nabla \cdot (\nu h \nabla \mathbf{u})}{h} \quad (6)$$

$$\eta_t + \nabla \cdot (h\mathbf{u}) = 0 \quad (7)$$

where  $\mathbf{u}$  is the velocity,  $\mathbf{f}$  is the vertical Coriolis vector,  $\eta$  is the surface displacement,  $r$  is the linear bottom drag coefficient,  $h$  is the total water depth ( $h = d + \eta$ ,  $d$  being the resting depth),  $\nu$  is the viscosity, and  $\bar{\eta}$  is the surface displacement of the equilibrium tide.

SEOM is based on the spectral element method, which can be categorized as an  $h$ - $p$  type finite element method, where accuracy is improved by increasing the number of elements ( $h$ -refinement) and/or increasing the interpolation order within each element ( $p$ -refinement). Truncation errors decrease at a high-order algebraic rate in the first case and exponentially fast in the second.

The solution procedure starts with the variational form of Eqs (6) and (7). The domain of interest is then subdivided into quadrilateral isoparametric and conforming elements contained in  $C^0$ , each of which contains a spectral grid based on the Gauss–Lobatto roots of the Legendre polynomials. The basis and trial functions in each element are the Legendre cardinal functions. We note that the interpolation order of the surface displacement is reduced by a factor of two with respect to the velocity interpolation to prevent the growth of spurious pressure modes. Substitution of the basis and trial functions in the variational formulation and evaluation of the ensuing integrals with Gauss–Lobatto quadrature produces a system of ordinary differential equations, which is integrated in time using a third-order Adams–Bashforth scheme. The coincidence of collocation and quadrature points yields a diagonal system of equations, which can be inverted easily and which simplifies considerably the time-integration procedure.

Figure 1 shows the spectral element grid used to discretize the World Ocean. The grid contains 1994 elements. With sixth-order polynomials to interpolate the velocity  $\mathbf{u}$  and fourth-order polynomials for the surface displacement  $\eta$ , the resulting nodal resolution averages  $2^\circ$  in the Indian Ocean,  $1^\circ$  in the Pacific and South Atlantic Oceans,  $0.5^\circ$  in the North Atlantic Ocean and  $1/3^\circ$  in the Arctic Ocean. Note that only the elemental grid is reproduced in Fig. 1; the interior mesh of collocation points within each element, 6 by 6 for velocity and 4 by 4 for surface height, has been omitted for clarity.

Dissipation in the model is provided by a linear bottom drag and a horizontal viscous term of Laplacian (harmonic) type. In the central experiment, the bottom drag coefficient  $r$  is set to  $10^{-3}$  m/s, yielding a spin-down time of  $\approx 46$  days for  $h = 4000$  m. The lateral viscosity coefficient is assumed to scale linearly with the maximum length of each element. (Grid Reynolds numbers are therefore approximately constant across the variable mesh.) The resulting viscosity coefficient varies from a minimum of  $760 \text{ m}^2/\text{s}$  to  $11,770 \text{ m}^2/\text{s}$  in the central experiment. The

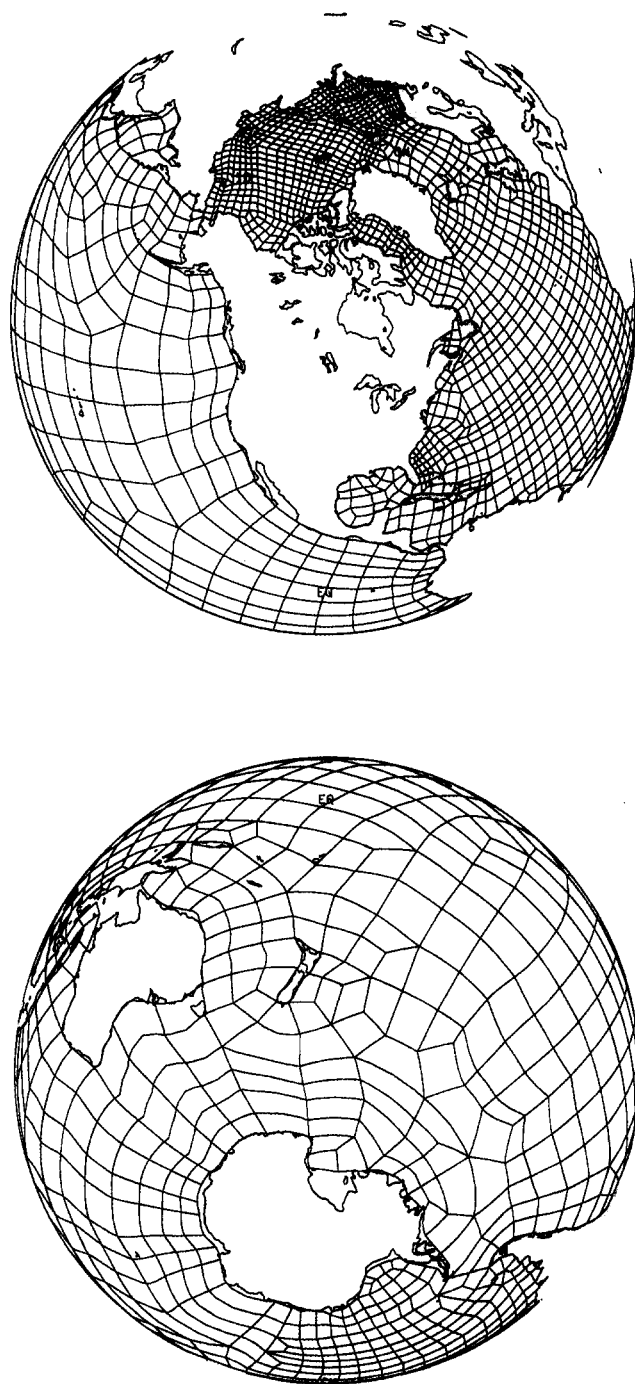


Fig. 1. Two views of the spectral element grid: (a) the northern hemisphere, and (b) the southern hemisphere. Only the quadrilateral elements and not the interior collocation nodes are shown.

time-step in the model is 20 s for all simulations. Integration is first performed for five periods to reduce transients created by the start-up; a sixth period is then computed and archived every 6 h for subsequent analysis. The bathymetry is interpolated, with light smoothing, from the ETOPO5 data set.

All major ocean basins are included. A passage simulating Bering Strait is included, but is wider than the real strait. The model strait has a depth of 50 m. Indonesian passages are included, with the same caveat. BARNIER (1988) has shown that barotropic Rossby waves tend to reflect from shelf-like geometries; this behavior suggests that failure to well-resolve the shelf areas should not have a first-order effect on the solutions or their dissipation. Details can, however, matter and the shelves require a more detailed examination; if they are important, dissipation would likely increase over our present estimate.

Equilibrium tide is given by the real form of Eq. (1):

$$\eta = H(1 - 3 \sin^2 \phi) \cos(\sigma t) \quad (8)$$

where  $\phi = \pi/2 - \theta$  is latitude,  $H = 2.1$  cm, and  $t$  is time relative to the time origin. Note that  $\bar{\eta}$  vanishes at  $\phi_c = \pm \sin^{-1}(\sqrt{1/3}) = \pm 35.3^\circ$ . The frequencies are here taken to correspond to periods of either 14 or 28 days—as in the spirit of our focus on the physics, the precise Mf and Mm periods are of only secondary interest. The response of the ocean's surface  $\eta$  is represented by an amplitude and phase:

$$\eta = \eta_0(\theta, \lambda) \cos(\omega t - \beta(\theta, \lambda)) \quad (9)$$

Because the system is linear, we can write

$$\eta = \bar{\eta} + \Delta\eta \quad (10)$$

where  $\Delta\eta$  is the anomaly relative to equilibrium (recall Eq. (3)).

The full shallow water equations are used, rendering the model nonlinear. A test was made of dynamical linearity by computing the magnitudes of the velocity as a function of position at the first overtone (7-day period) of the forced motion. A map (not shown) of the result produced amplitude ratios nowhere exceeding  $10^{-2}$  and, in general, were much smaller than that. We conclude that to a very good approximation, the tidal response in the model is linear.

### 3. RESULTS

A number of numerical experiments were run; Table 1 lists those we will focus on here. Observational results are expressed often as complex admittances—the ratio of response to forcing. This form has advantages for data analysis discussed in WUNSCH (1967). A disadvantage is the vanishing of the forcing potential at  $\phi = \phi_c$ . With a model producing essentially spatially continuous, noise-free output, there is some advantage instead to examining the anomaly  $\Delta\eta$ . In contrast to the earlier studies, however, we will focus here in large part on the velocity field implied by the model solution. The elevation over much of the ocean is visually dominated by the equilibrium contribution, while it is the comparatively small elevation gradients, which produce the dynamically important velocities. Note that for equilibrium tide (which cannot be an exact result except asymptotically as  $\sigma \rightarrow 0$ , because there must be some water movement, no

Table 1. Different model runs alluded to in the text

Run	Orig. description	Description	Viscous dissipation	Bottom dissipation	Total dissipation	Tidal work	PE	KE	$Q$
1	17	Std. exp (14 d Mf)	3.21	2.25	5.46	5.45	2.29	2.87	5.0
2	16	2 × bottom drag	2.26	3.29	5.55	5.54	2.29	2.15	4.2
3	21	2 × viscosity	3.70	1.82	5.51	5.50	2.28	2.30	4.4
4	23	1/2 × viscosity	2.68	2.73	5.41	5.42	2.28	3.50	5.6
5	22	Smoothed bathy	3.29	2.42	5.71	6.17	2.28	3.15	5.0
6	19	No Arctic	2.09	1.25	3.34	3.30	1.97	2.32	6.7
7	25	28 d. Mm	1.11	0.77	1.88	1.88	2.46	0.88	4.7
8	24	1/2 × visc (Mm)	0.96	0.93	1.89	1.88	2.46	1.09	4.9

Viscous, bottom, total dissipation and tidal work are in units of  $10^8$  W, under the assumption of a fluid density of  $10^3$  kg/m<sup>3</sup>. Potential (PE) and kinetic (KE) energies are in units of  $10^{14}$  J.  $Q$  is defined in the text as the "quality factor" for a harmonic oscillator system. Changes in different experiments are all relative to run number 1. Potential energy of equilibrium tide is about  $2.7 \times 10^{14}$  J.

matter how slight, to generate the elevation changes), the velocity field is formally zero. Thus, the structure and magnitude of the velocity field is an immediate measure of non-equilibrium behavior.

Run 1, as listed in Table 1, is our reference or standard solution corresponding nominally to the Mf solution with realistic topography, geometry and reasonable values for the dissipation coefficients. Figure 2 shows  $|\Delta\eta|$  and its phase (relative to equilibrium) for the entire globe for a solution which appears fairly realistic. Over much of the tropical Pacific, the phases lie near  $180^\circ$ , serving to reduce the total amplitude relative to equilibrium as the tide gauges appear to show (MILLER *et al.*, 1993; Fig. 1). Little small scale structure is observed (the velocities in Fig. 3 are a measure of the gradients) except in the western tropical Pacific suggesting that whatever small scale Rossby waves are excited here tend to be damped heavily away from the western boundary. To some degree, this solution vindicates all of the previous descriptions of the tidal response: there is clearly a large-scale structure present, along with a superposed small scale most conspicuously on the western sides of the ocean basins, and identifiable as a Rossby wave contribution.

Elsewhere, visually, there are a few major features: (1) The Southern Ocean (where almost no tide gauge records are available) displays a complex structure, evidently partly, but not wholly, associated with the topographic system there (compare to SEILER, 1990, Fig. 7). Anomaly amplitudes approach 1 cm but are typically closer to 0.5 cm. (2) The Atlantic shows a distinct westward intensification only weakly evident in the Pacific Ocean. (3) The Arctic response has both a large amplitude ( $\approx 1$  cm) and phase lag (typically  $30$ – $40^\circ$ ), with large phase changes in the passages to the ocean further south. The Arctic tidal amplitude results are complex and interesting. Apparently the topography of this basin produces regional amplification. Phases here are more uniform than the amplitudes, lying near  $180^\circ$ .

Figure 3 shows the corresponding zonal and meridional velocities at  $t = 70.25$  days, a velocity field which is nearly in geostrophic balance with the elevation field and which is visually tightly bound to the gradients in Fig. 2, although the eye does not readily detect the large-scale features



Fig. 2. Amplitude (a) in mms. Equilibrium amplitude was 2.1 cm. The color discontinuity in the South Pacific in phase is an artifact of the phase wrap from  $-180$  to  $+180^\circ$  and must occur somewhere in such a plot.

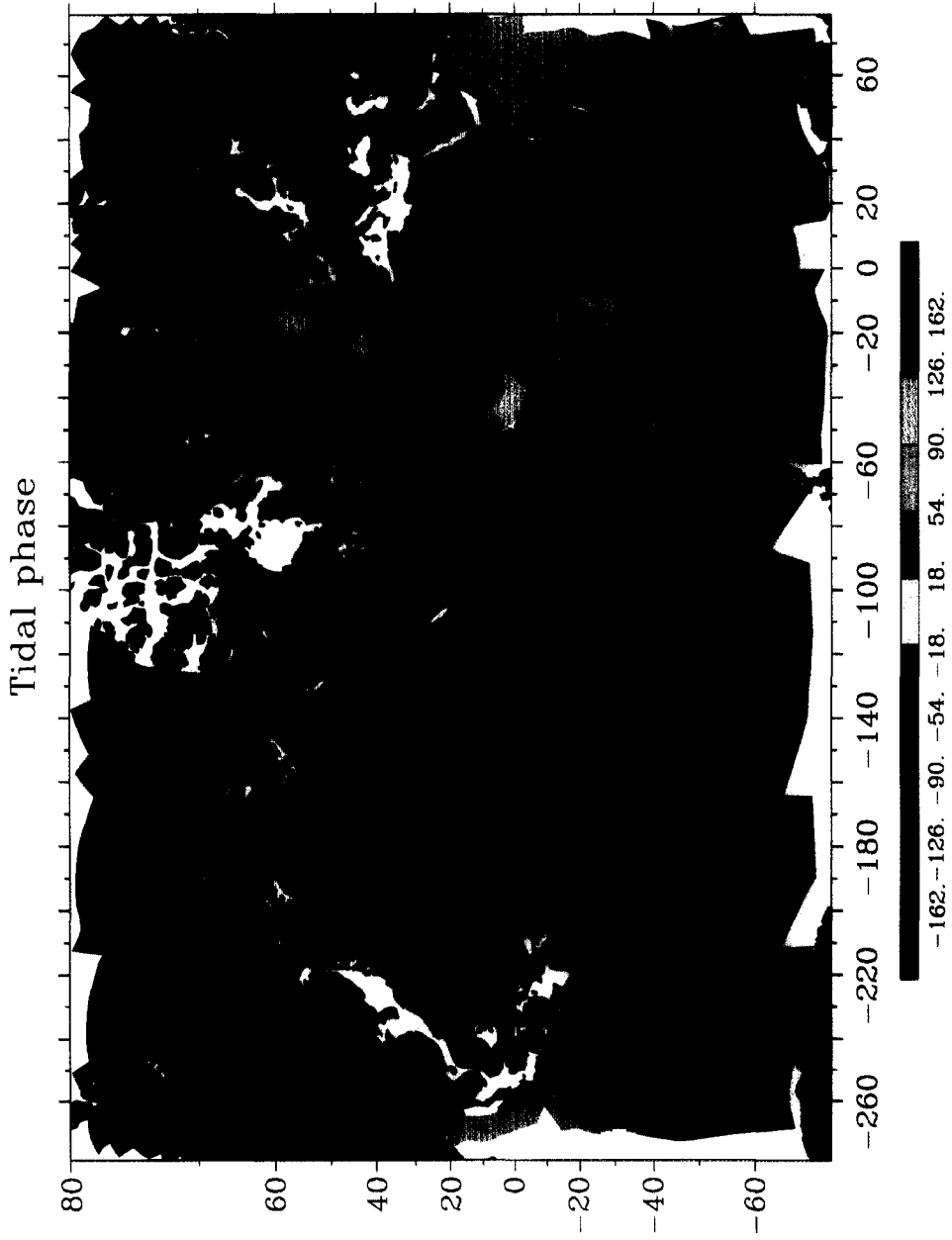


Fig. 2. Phase lag (b) in degrees of the elevation anomaly  $\Delta\eta$  relative to equilibrium tide of run 17. Equilibrium amplitude was 2.1 cm.

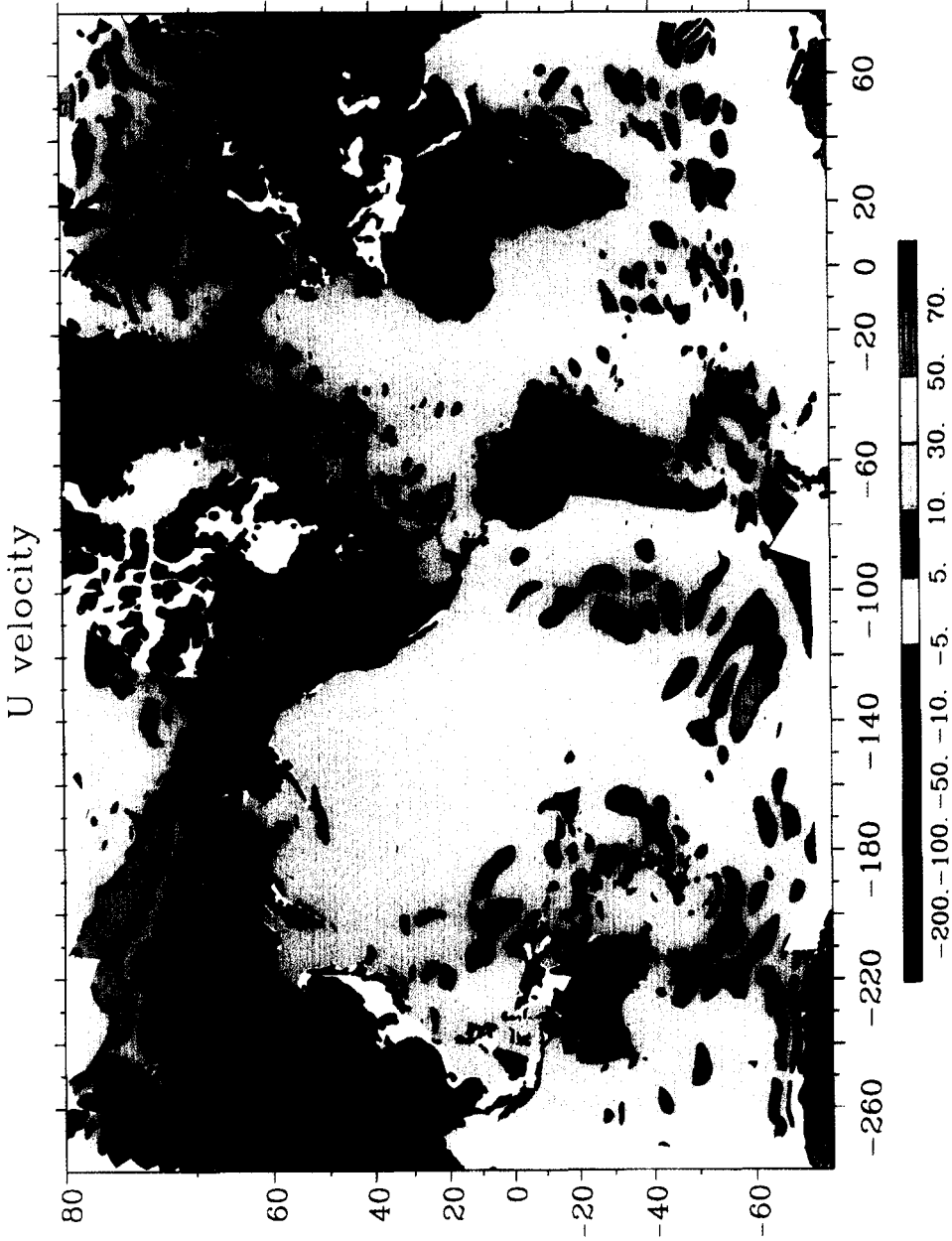


Fig. 3. (a)  $u$  components of velocity at  $t = 70.25$  days for experiment 17; the units are in  $10^{-1}$  mm/s. Necessarily in a nearly geostrophic system, the velocities are essentially determined by the gradients of the field in Fig. 2.

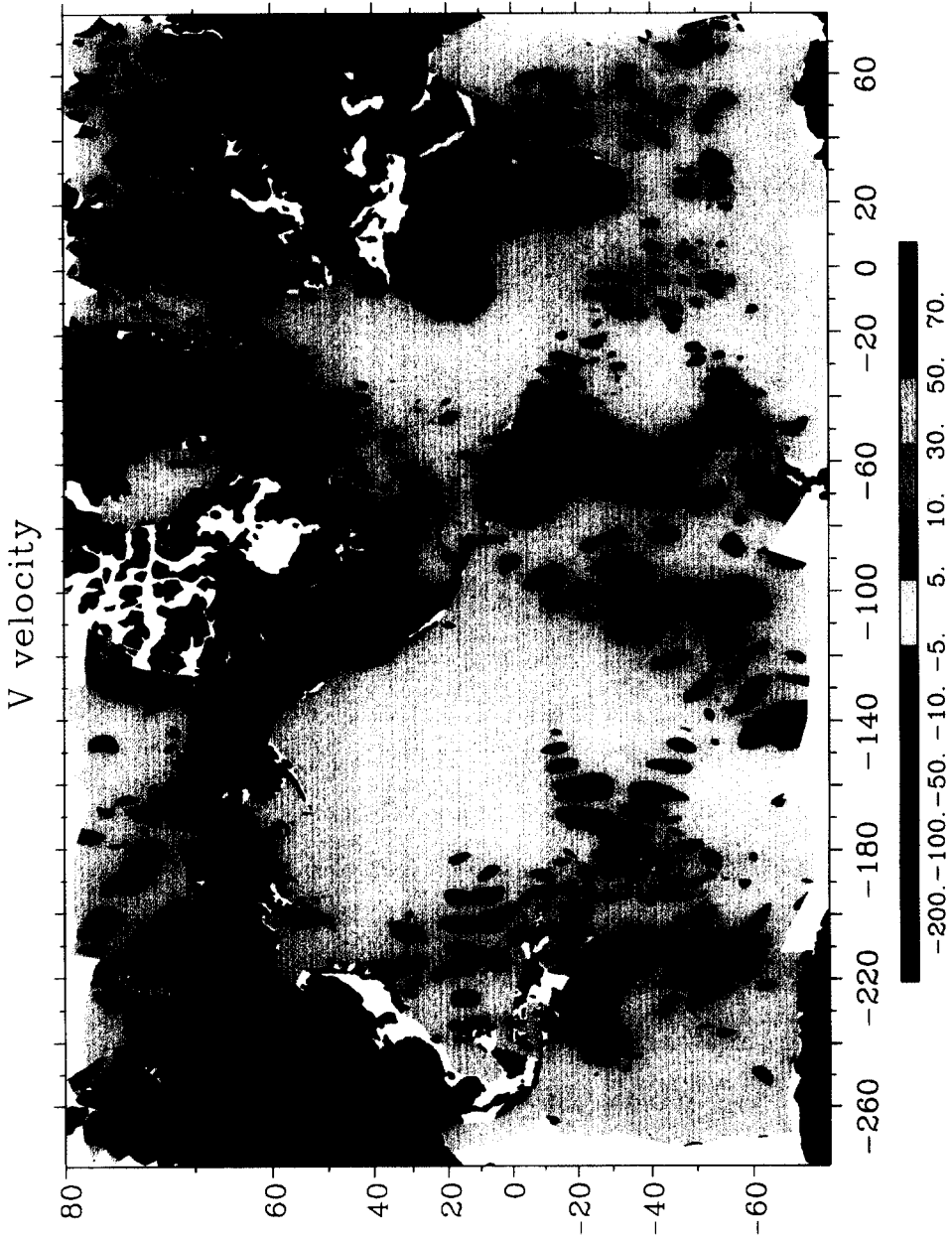


Fig. 3. (b)  $v$  components of velocity at  $t = 70.25$  days for experiment 17; the units are in  $10^{-1}$  mm/s.

associated with weak meridional pressure gradients. A general westward intensification, consistent with the simplest Rossby wave behavior in the presence of dissipation (WUNSCH, 1967), is clearly present.

#### 4. ENERGY AND DISSIPATION

If the nominal Mf solution is accepted as realistic, the most interesting elements are the dissipation rates and distribution. At a single point, the total energy per unit mass is

$$T = \frac{1}{2} h(\theta, \lambda)(u^2 + v^2) + \frac{g}{2} \eta^2 \quad (11)$$

the first term being the kinetic and the second the potential energy/per unit mass. Averaging over one cycle, and integrating over the ocean (the area element being  $dA = a^2 \sin \theta d\theta d\lambda$ ), the kinetic,  $T_K$ , and potential energies,  $T_P$ , tabulated in Table 1 are respectively about  $2.3 \times 10^{14}$  and  $2.2 \times 10^{14}$  J (using a water density of  $1000 \text{ kg/m}^3$ ). For reference, the potential energy of equilibrium tide is about  $2.7 \times 10^{14}$  J and thus the tidal response has a smaller potential energy than does the equilibrium tide. This result is best interpreted as showing that part of the dynamical response occurs on a very large scale and acts to render less than equilibrium the elevation response proportional to the  $Y_2^0$  term in the forcing.

The ratio of kinetic to potential energy in Rossby waves is a function of the wavenumber content of the waves. In the geostrophic limit,

$$\frac{T_K}{T_P} = \frac{gh}{f^2} (k^2 + l^2) \quad (12)$$

Taking  $gh/f^2 = 9.4 \times 10^{12}$ , one has approximate mid-latitude ( $h = 5000 \text{ m}$ ,  $2\pi/f = 1 \text{ day}$ ) equipartition if  $k^2 + l^2$  corresponds to a very long mean wavelength of about 19,000 km. Thus, the near equipartition of energies shows that the potential energy is dominated by the equilibrium component,  $\bar{\eta}$ , which has a very long spatial scale but generates almost no flow, while the smaller dynamical response scales are dominated by the kinetic energy.

The Laplace tidal equations are readily manipulated (e.g. TAYLOR, 1919; GARRETT, 1975) to produce an energy balance when integrated over a full tidal period of

$$\frac{\oint gh \langle \eta \mathbf{u} \rangle \cdot \mathbf{n} dl}{1} = \frac{\int gh \langle \mathbf{u} \cdot \nabla \bar{\eta} \rangle dA}{2} + \frac{\int h \langle \mathbf{u} \cdot \mathbf{F} \rangle dA}{3} \quad (13)$$

Here the bracket denotes the period average, the area  $A$  is any horizontal region, whose unit outward normal is  $\mathbf{n}$ , and  $\mathbf{F}$  represents any forces—here generally the dissipation terms, rendering  $\mathbf{F}$  negative. Term 1 is the net flux in or out, term 2 is the work done in the volume interior by the horizontal pressure forces of the equilibrium tide, and the third term is the direct interior dissipation. If one uses

$$h \mathbf{u} \cdot \nabla \bar{\eta} = \nabla \cdot (h \bar{\eta} \mathbf{u}) - g \bar{\eta} \nabla \cdot (h \mathbf{u}) \quad (14)$$

Eq. (13) becomes

$$\frac{\oint gh\langle\eta\mathbf{u}\rangle\cdot\mathbf{n}dl}{1} = \frac{\oint gh\langle\bar{\eta}\mathbf{u}\rangle\cdot\mathbf{n}dl}{2} + \frac{g\int\bar{\eta}\frac{\partial\eta}{\partial t}dA}{3} + \frac{\int h\langle\mathbf{u}\cdot\mathbf{F}\rangle dA}{4} \quad (15)$$

The work by the moon (term 3) is now given in terms of the equilibrium elevation itself and the net energy flux out of the volume involves a flux of equilibrium energy (term 2), the one omitted by TAYLOR (1919) and corrected by GARRETT (1975). A criterion used to test for model convergence was that the sum of the two dissipation terms in Table 1 should equal to high accuracy the net work by the moon.

Figure 4 displays for nominal Mf the distribution of kinetic energy/unit mass, the two contributors to the dissipation and the distribution of work by the moon on the ocean. As a rough generalization, kinetic energies and dissipation are high in the Southern Ocean extending into the South Atlantic and Pacific, in the western and high latitude North Atlantic. Generally speaking, the regions of high dissipation correspond to strong input of energy by the moon into the ocean—suggesting that most energy is dissipated locally, rather than being transmitted over long distances, in contrast to (e.g. LYARD and LE PROVOST, 1997) the semi-diurnal tides. The strong spatial variability of the tidal elevations leads to a complex juxtaposition of regions where the net work is by the ocean on the moon with those of net work by the moon on the ocean. The sum is necessarily dominated by the latter.

The global dissipation is found to be nearly  $0.5 \times 10^9$  W (0.5 GW). Thus, with the total energy quoted above, the “quality factor”,  $Q$  is (JACKSON, 1975),

$$Q = 2\pi \frac{E}{\dot{E}T} \approx 5 \quad (16)$$

where  $E$  is the total energy,  $\dot{E}$  is the average energy dissipation rate, and  $T = 14$  days. A  $Q$ -value of 5 is roughly consistent with, but lower than, estimates made for the ordinary tides. More significantly, it is indistinguishable from the value obtained by LUTHER (1980) for an apparent 5-day normal mode of the Pacific Ocean and one of the few other available direct estimates of low frequency ocean dissipation. (From the crude GEOSAT measurements, CARTWRIGHT and RAY, 1990, estimated  $Q \approx 7.8$ .) On the global average,  $Q = 5$  implies that all of the energy in the tide would dissipate in about 11 days—significantly less than one period. A strong conclusion then is that for barotropic motions, the average ocean is a very heavily damped system and large-scale, clear modal excitation does not occur.

## 5. CHANGING PARAMETERS

A number of experiments were carried out to elucidate the long-period response more generally. These experiments included variations in the dissipation parameters, in the tidal period, in the topography, and owing to the MILLER *et al.* (1993) conclusions, in the connections to the Arctic Ocean. We will treat these results in mainly summary fashion although a great deal of detail is visible in the changes from the standard model.

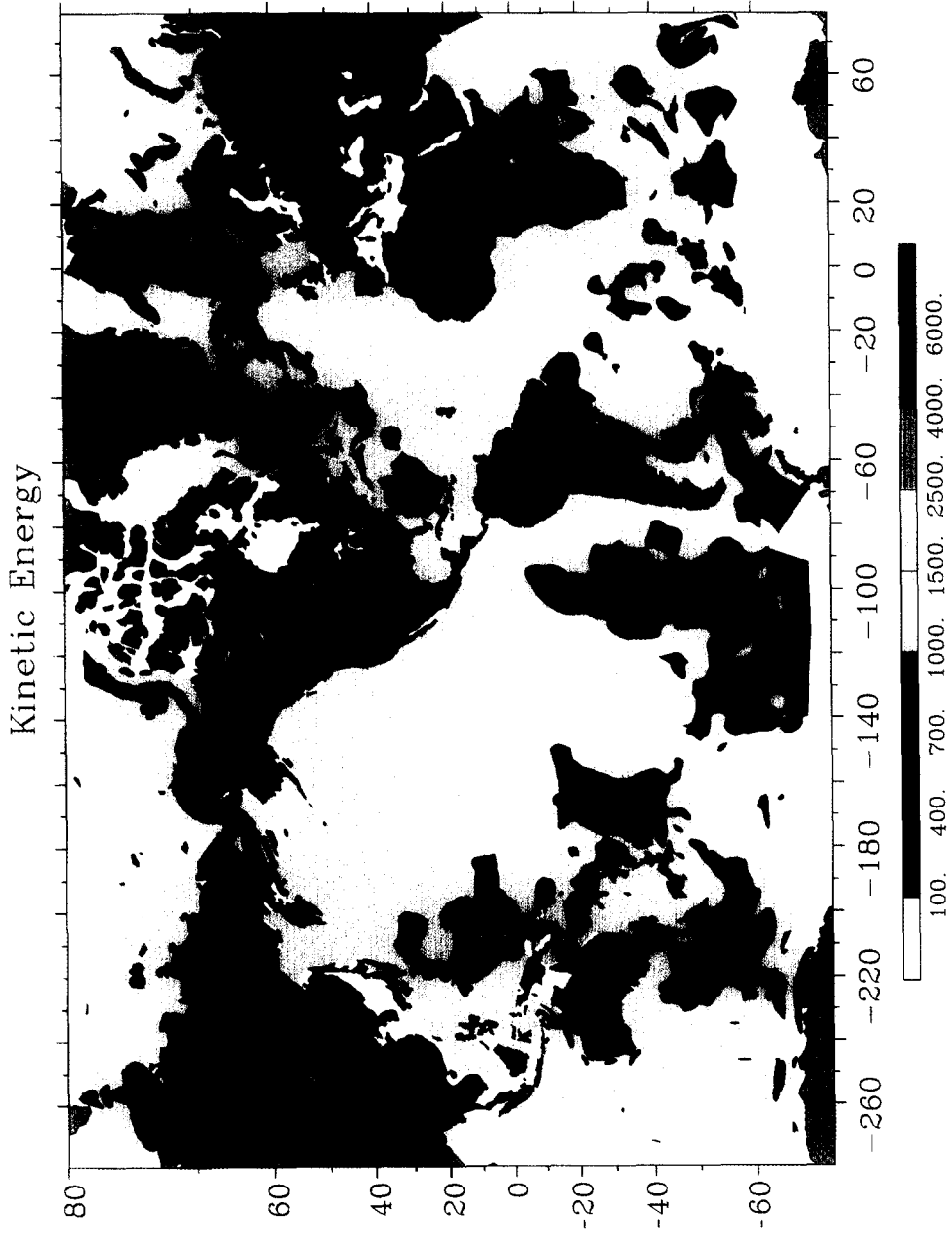


Fig. 4. (a) KE distribution in run 17, in  $10^2 \times \text{J/m}^2$ .

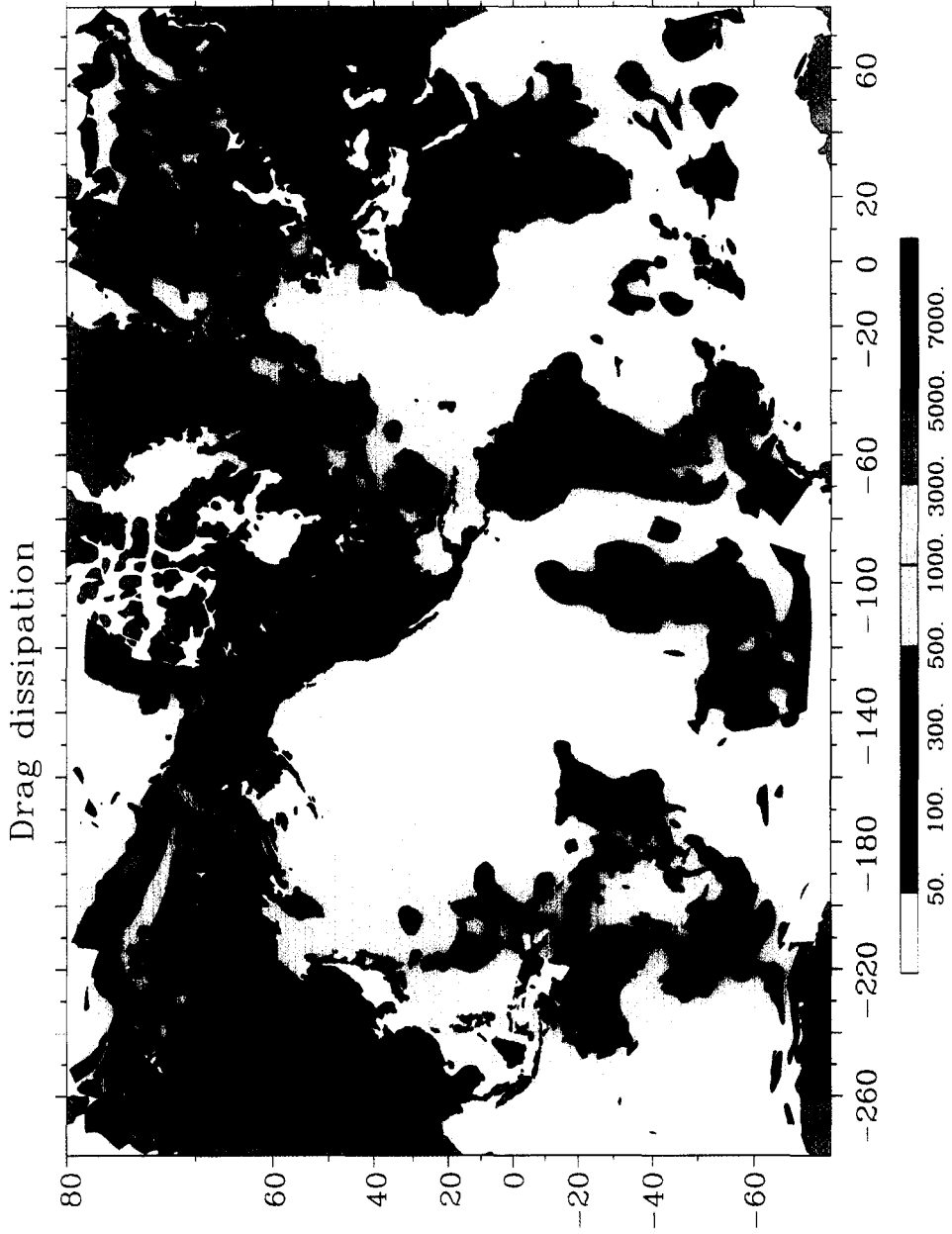


Fig. 4. (b) Bottom drag dissipation in  $10^8 \times W/m^2$ .

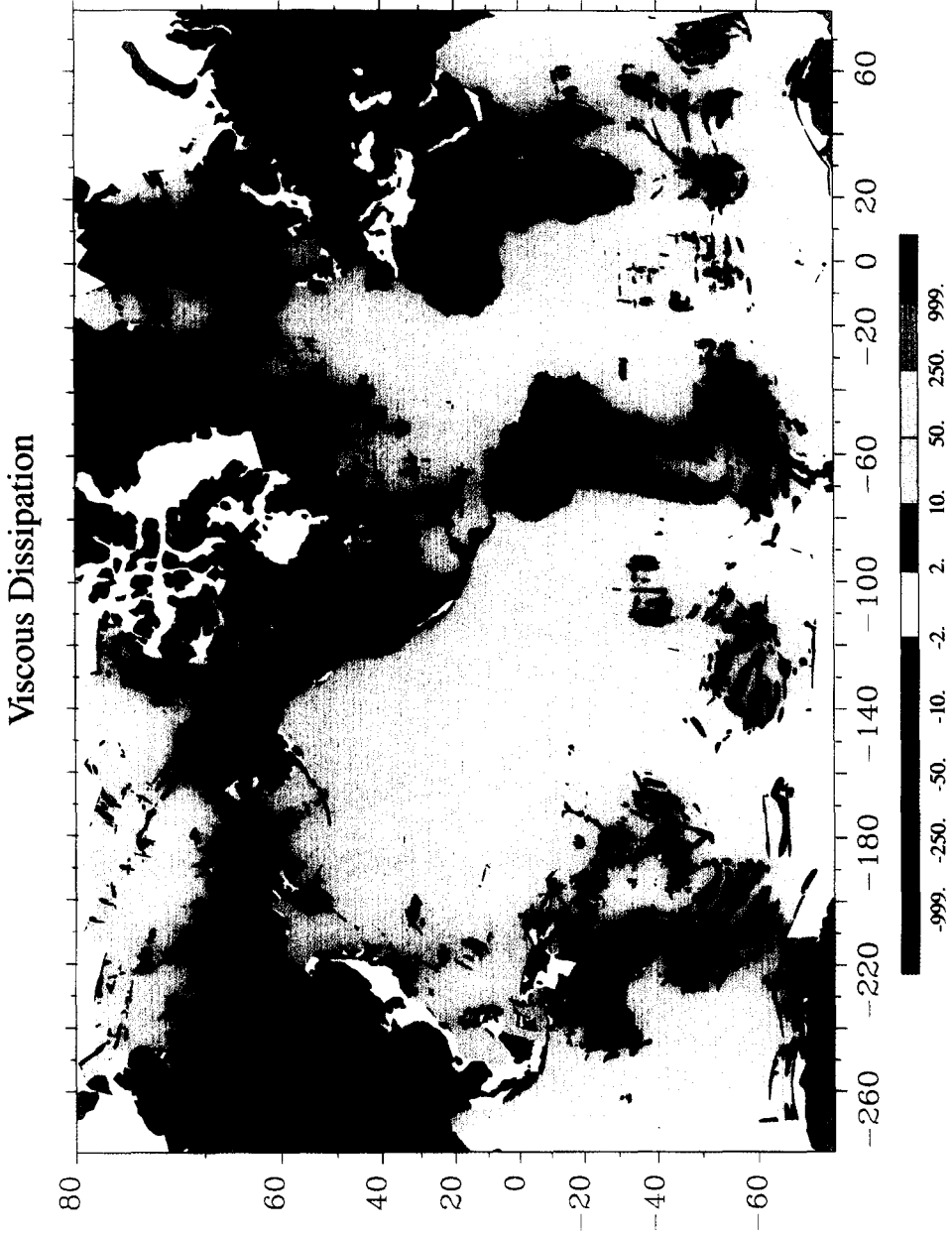
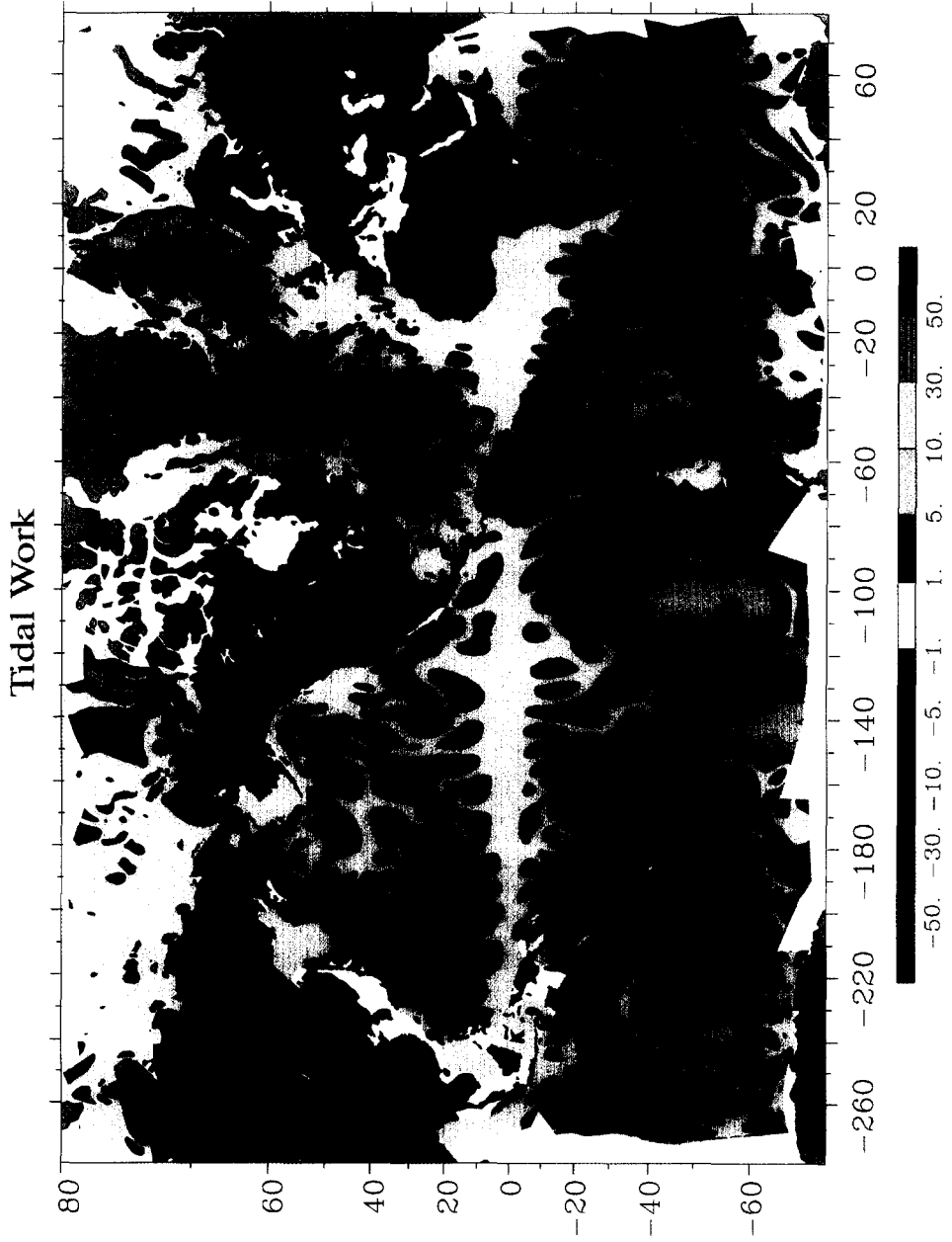


Fig. 4. (c) "Viscous" dissipation in  $10^6 \times W/m^2$ .



### 5.1. Variations in dissipation parameters

Experiment 2 was run using a doubled bottom friction coefficient, all other parameters remaining the same. As can be seen from Table 1, the total dissipation and hence the  $Q$  hardly changed, but the ratio of viscous to bottom drag dissipation did change significantly. The ratio of kinetic to potential energy was reduced—consistent with a reduced dynamical response. Visually, the fields of tidal work and bottom dissipation are largely unchanged from the central experiment in their spatial distributions. In experiment 3 the viscous coefficient was doubled, the bottom friction coefficient remaining as in experiment 1. Once again the total dissipation and  $Q$  hardly changed but one now has near equality in kinetic and potential energy. The net dissipation thus seems fairly robust, despite changes in the contributions to the system energy and dissipation mechanisms.

### 5.2. Closing the arctic

To investigate the suggestion of MILLER *et al.* (1993) that the Arctic Ocean might play an important role in regulating tidal response in the Pacific Ocean, we have repeated the central experiment on a global grid that omits the Arctic Ocean. The time- and volume-averaged statistics (experiment 6, Table 1) do in fact show an influence from the exclusion of the Arctic; in particular, tidal work and bottom dissipation values are greatly reduced, though the resulting  $Q$  is enhanced only slightly. Most important, however, the diagnostic measures discussed here (tidal amplitude and phase, kinetic energy, etc.) show no major change in spatial structure or amplitude in the Pacific, or for that matter over the majority of the globe with the exception of the western North Atlantic (Fig. 5).

The Laplace tidal equations are sensitive to lateral boundary conditions, and the closing of the Arctic would be expected to generate a complex shift in the solution overall. But in addition to this dynamical response, the tidal equations admit the addition of a simple spatially constant, time-varying component to any solution

$$\eta \rightarrow \eta + C \quad (17)$$

where the numerical value of  $C$  is determined by mass conservation

$$\iint_{\text{ocean}} (\eta + C) dA = 0 \quad (18)$$

Removal of the Arctic changes the dynamical boundary condition for the remaining ocean, but also the oceanic volume and hence the value of  $C$ . It is not possible to separate the dynamical changes from the kinematic ones, but the observed large-scale changes in amplitude and phase are approximately consistent with the changes forced by the volume reduction. We conclude from experiment 6 that, although the Arctic contributes substantially to the global budget of tidal energy in the Mf band, it does so primarily locally, without substantial remote effect on tidal response elsewhere except for the overall shifts expected from mass conservation.

### 5.3. Smoothing the bathymetry

Experiment (5) was conducted to examine sensitivity to further smoothing of model bathymetry. The procedure, whose details will not be reported here, involved a higher degree of spectral

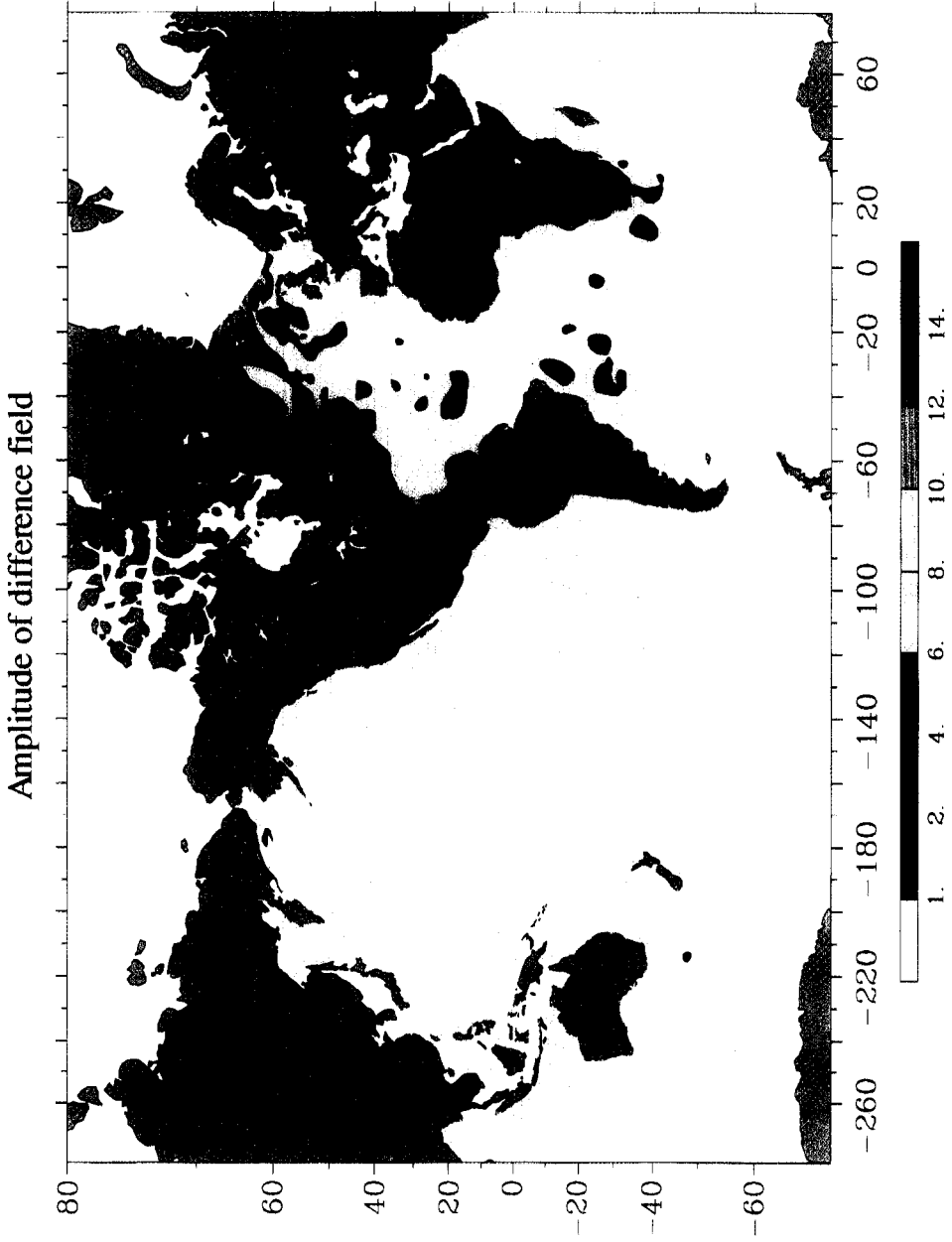


Fig. 5. Amplitude (a) of the difference in the solutions with an Arctic and without an Arctic Sea in the model.

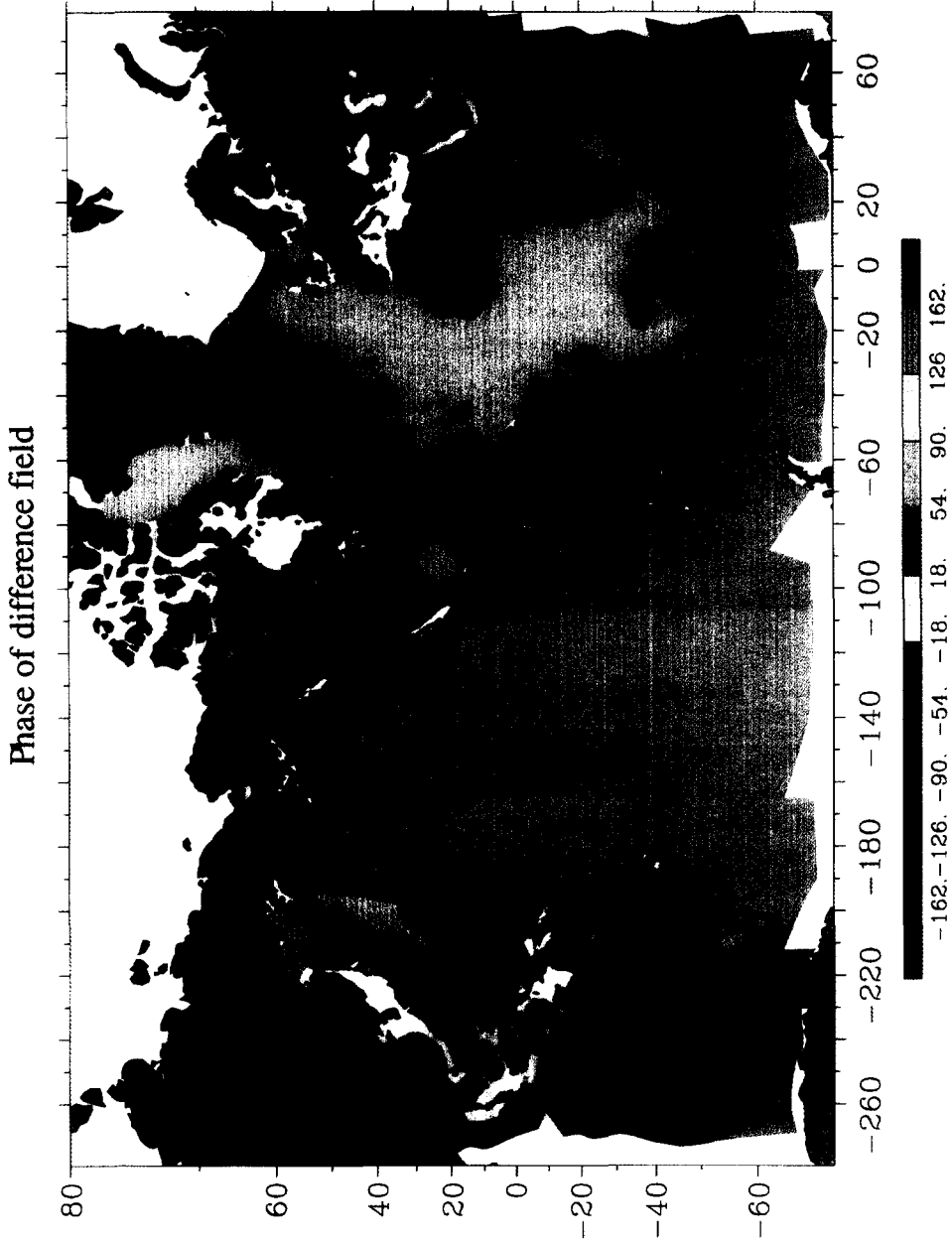


Fig. 5. Phase (b) of the difference in the solutions with an Arctic and without an Arctic Sea in the model.

smoothing to the topography within each element than was used for the central experiment. Perhaps contrary to expectation, the net energy production by tidal forces (and of course the total dissipation) are *increased* with the smoother bathymetry (Table 1), though  $Q$  is not influenced. Neither are the spatial patterns of energy gain and loss significantly affected. This behavior might be expected, e.g., from the work of BARNIER (1988), who found that barotropic waves tend to be strongly reflected from regions of depth change, once a steepness threshold was reached so that the smoother topography permits the wave motion to enter shallow, higher dissipation regions.

#### 5.4. Changing the period: Mm

The lunar monthly tide has a period near 28 days, and has about half the amplitude of the fortnightly term. The observational literature is divided on whether it is closer to equilibrium than is Mf, as simple limiting theories suggest it should be. In experiment 7, all parameters of the standard experiment (1) were retained (including the amplitude) except that the tidal period was doubled. The visual change in the spatial patterns is again not striking in either amplitude or phase, though the overall levels of the former are reduced by about 50% over the central experiment. Again the system is highly damped. The tide is dominated now by the potential energy consistent with the presence of longer wavelengths, more relative potential energy, and a general shift toward a more nearly equilibrium response. ( $Q$ , as we have defined it here, would be infinite for a completely equilibrium tide: there would be a finite energy in the equilibrium response and no dissipation; pure equilibrium tide can only exist in the limit as  $\sigma \rightarrow 0$ . A  $Q'$ , based solely upon the kinetic energy, can be deduced readily from Table 1, however.)

## 6. EFFECT ON LUNAR ACCELERATION

Tidal dissipation affects the lunar orbit as well as the earth's rotation. MUNK and MACDONALD (1960), LAMBECK (1980), etc. discuss the general problem in detail. Dissipation of the long-period tides contributes a small component to the overall tidal dissipation effect. Calculation of the effects on the lunar orbit has generated an opaque literature: CHRISTODOULIDIS, SMITH, WILLIAMSON and KLOSKO (1988) and MARSH *et al.* (1990) conclude that like the other tidal constituents, the long-period components accelerate the moon in its orbit, and slow the earth. In contrast, CHENG, EANES and TAPLEY (1992) found that, surprisingly, dissipation of the long-period tides brakes the moon and actually accelerates the earth's rotation!

An heuristic explanation for this last conclusion appears to be as follows (R. EANES, personal communication, 1996): the earth's rotation is not directly relevant to the derivation of the forcing potential for the long-period tides, but depends only on the orbital period and the lunar orbital inclination. That is, the form and period of the long-period constituents is independent of the rotation rate. For these constituents, the moon (or sun) can be thought of as orbiting a non-rotating earth in a plane with the appropriate inclination to the equator. Then the tidal "bulge" lags behind the orbiting moon thus decelerating it in its orbit (bringing it closer to the earth), and by angular momentum conservation, the earth's rotation must accelerate. ("Bulge" must be interpreted loosely: consider the case of a water-covered earth; the oceanic response is then zonally symmetric, but the elevation would lag the orbiting moon.) But this argument is qualitative, and a quantitative resolution of the conflicting conclusions is still needed.

In any event, the inferred Mf dissipation rate of 0.5 GW is less than 0.1% of that inferred

---

for the other tidal constituents (of order 3.5 TW); the change in the lunar motion is thus very small and, at the present time, primarily of theoretical interest.

## 7. COMPARISON WITH OBSERVATIONS

As we have said, our present purpose is not an attempt at a detailed reproduction of the observations, but rather to gain insight into the major physics of the long-period tides. Nonetheless, one needs to understand whether the model has been run in a physical regime consistent with what is known of the oceanic response.

The chief difficulty in this subject is the low signal-to-noise ratio of the tidal response to the background variability in sea level records spanning a few years and, in the pre-satellite era, of the maldistribution of island tide gauges. The early estimates from tropical tide gauges by WUNSCH (1967) were based upon comparatively short (4 years at most) records and led to very large (if still optimistic) error bars.

Much longer records (and the FFT algorithm) were available to MILLER *et al.* (1993) who tabulated estimates of Mf parameters from low-latitude Pacific tide gauge stations. Both in amplitude and phase the island observations are comparable to those seen in the standard model results for the tropical Pacific (the self-attraction and load effects are approximately a 15% effect not included in the model; see HENDERSHOTT, 1972; AGNEW and FARRELL, 1978).

There are now sufficient TOPEX/POSEIDON altimetry data to estimate long-period tidal parameters. TOPEX/POSEIDON-derived estimates for Mf have been provided by DESAI and WAHR (1995), S. DESAI (personal communication, 1995, 1996) and L. KANTHA (personal communication, 1996). A summary would be that there is rough quantitative agreement between the standard model and these various estimates. For example, Fig. 6 (S. DESAI, personal communication, 1996) shows the corresponding smoothed TOPEX/POSEIDON amplitudes. Again, a reasonable correlation with the model is evident, by eye.

The existing TOPEX/POSEIDON results are probably badly contaminated by background noise from the oceanic general circulation variability. There are two remedies: longer altimetric records should eventually raise the tidal signals arbitrarily far above the background noise-dependent only upon the record duration. More ambitiously, one could attempt to predict the oceanic variability in the TOPEX/POSEIDON data using a general circulation model driven by observed surface boundary winds and buoyancy fluxes. These estimates could then be subtracted from the altimetric data, and the tidal analysis done on the residuals. We expect that both routes will eventually be tried, and therefore a review such as this written a few years from now should be much more definitive than we can be.

## 8. EARTH ROTATION AND POLAR MOTION

The long-period tides contribute significantly to polar motion and length of day changes. All the solutions here are accompanied by computations of their contribution to these quantities, but for reasons of space will be reported elsewhere.

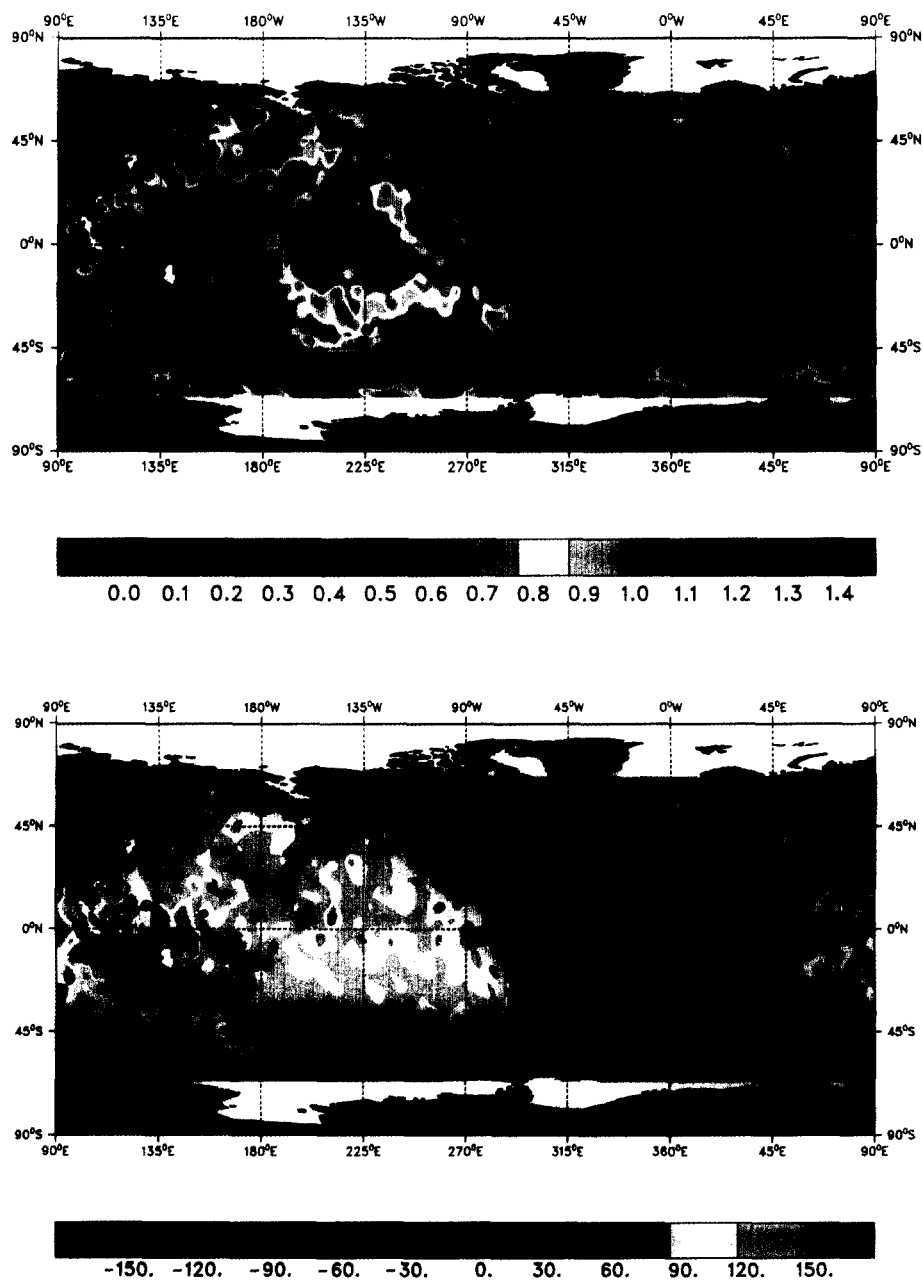


Fig. 6. Amplitude (a), and phase (b) of the Mf tidal anomaly  $\Delta\eta$  as computed by S. DESAI (personal communication, 1996), from TOPEX/POSEIDON altimeter data. These results must be regarded as preliminary as they are corrupted by contributions from the time varying oceanic general circulation.

## 9. THE POLE TIDE

The so-called pole tide is generated by the 14-month Eulerian free wobble (the “Chandler wobble”) of the earth’s rotation axis, which generates a corresponding change in the centrifugal potential at any point on the earth’s surface. The result is equivalent to a 14-month tide of amplitude about 0.5 cm with eastward-moving spatial structure corresponding to spherical harmonic  $Y_2^0(\theta, \lambda)$ , but having the character of a narrow-band random process rather than a pure line frequency. Extended discussions of the wobble can be found in MUNK and MACDONALD, 1960, LAMBECK (1980); LAMBECK, (1988)) and in many review articles. Dynamically, we have seen that there is a tendency for the long period tides to become more equilibrium as the period lengthens. Various theoretical analyses of this problem have been carried out by WUNSCH (1986), CARTON and WAHR (1986), DICKMAN (1988) and others. Although there are some claims of deep ocean non-equilibrium pole tides, these are unconvincing in view of the very low signal-to-noise ratios and the clear implications of theory. The global data analysis of TRUPIN and WAHR (1990) is consistent with a deep water equilibrium tide.

HAUBRICH and MUNK (1959) apparently first noticed a peculiarly amplified response in the North and Baltic Seas appearing as a distinct spectral peak in sea level at the appropriate 14-month period. The available data were further analyzed by MILLER and WUNSCH (1973) who showed a greatly amplified response relative to equilibrium, striking amplitude growth to the east, along with an apparent phase propagation to the east. This response is difficult to rationalize.

As an explanation, WUNSCH (1986) suggested that, coincidentally, there was a travelling wave resonance to an eastward propagating topographic Rossby wave (eastward because the North Sea shoals southward, thus reversing the sign of the net  $\beta$ -effect). More recently, TSIMPLIS, FLATHER and VASSIE (1994) claimed that the spectral peak in sea level was essentially an atmospheric phenomenon-driven in the ocean by a narrow-band peak in atmospheric forcing at the pole tide period. XIE and DICKMAN (1996) show evidence that the eastward intensified motion is not temporally stable—a result consistent with a stochastic excitation by the atmosphere. A rationalization as an atmospheric peak, however, is even more difficult to accept than the idea of a coincident resonance in the North Sea. Maintenance of a narrow-band energy peak in atmospheric variables in the restricted region of the North Sea is counter to the known behavior of the lower troposphere and the atmospheric spectral peak in TSIMPLIS *et al.*’s Fig. 4 is neither statistically significant, nor of as high  $Q$  as the one observed in oceanic sea level. (The direct atmospheric response to the *gravitational* forcing by the pole tide would be minute.) On the other hand, MILLER and WUNSCH (1973) reported significant coherence between tide gauge stations with a simple phase shift eastward across the North Sea. This result is difficult to reconcile with a purely atmospherically driven motion. MILLER and WUNSCH (1973) did note, however, that the background continuum did manifest much the same structure as the apparent pole tide.

Thus, the enigma appears to have deepened. But an explanation exists consistent with all these phenomena: that there is indeed a resonant mode of the North Sea precisely at the pole tide frequency, excited by *both* meteorology and the pole tide. This conclusion appears to account for all the data analyses including those of MILLER and WUNSCH (1973), TRUPIN and WAHR (1990) and XIE and DICKMAN (1996). The regression analysis of the latter authors appears to produce a non-equilibrium pole tide, but not one showing a robust eastward growth. Another troubling point is the failure of the storm surge model of TSIMPLIS *et al.* (1994) to show the resonance.

Overall, at the present time, it is probably best to state a negative conclusion: nowhere in the

world is there evidence of a non-equilibrium pole tide. The North and Baltic Seas remain a possible, but difficult, exception. The model used here for the Mf and Mm constituents could readily be employed for the pole tide period. The only difficulty is the pragmatic one of obtaining sufficient spatial resolution in the shallow seas to permit definition of the very short wavelengths at these periods implied by the dynamics.

## 10. DISCUSSION

The response at any given point of a barotropic ocean to forcing by a potential field at low frequencies is evidently a complex summation over motions generated both locally and propagating in from long distances, affected along the way by topographic scattering and dissipation. Mathematically, the summation over the hypothetical normal modes, Eq. (3), is a valid representation. But the picture that emerges from the present model is of a very heavily damped system, in which most input energy is dissipated locally and the modal structure is so complex as not to be particularly helpful.

MILLER *et al.* (1993) interpret their results as showing that a Kelvin wave emanating from the Arctic Ocean dominates the tropical Pacific Ocean. A barotropic Kelvin wave at 14-day period, in a water depth of 5000 m, would have a wavelength of about  $2.7 \times 10^5$  km, or about seven times the circumference of the earth. The resulting modal coefficient in Eq. (3),  $(l^2 - q^2)^{-1}$ , characterizing the response, will be finite (see, e.g., MORSE and FESHBACH, 1953) and the wave will be present. Many other gravity modes will also be present in greater or lesser amounts, but in view of the comments made above, however, about non-uniqueness, and the heavy dissipation present, the modal representation does not appear to be a clearly advantageous one.

Visually, the most active region for Mf and Mm is in the Southern Ocean. This feature appears quite conspicuously, e.g., in the earlier results of SEILER (1990). The tropical Pacific—where most of the tide gauge data come from—is, ironically, untypically simpler than most of the remaining global response. Some simple rationalization of the structure emerges from a study of the scale of barotropic Rossby waves. For a fixed frequency on a dissipationless mid-latitude  $\beta$ -plane, the horizontal wavenumbers of permissible free waves at fixed frequency,  $\sigma$ , must satisfy the relation,

$$k^2 + \frac{\beta k}{\sigma} + l^2 + \frac{f^2}{gh} = 0 \quad (19)$$

Here,  $(k, l)$  are the zonal and meridional wavenumbers respectively, and  $f$  is the local Coriolis parameter. Consider a flat-bottomed ocean in which the barotropic Rossby radius  $\sqrt{gh}/f \approx 1800$  km (appropriate to an ocean of about 4000 m depth at about  $50^\circ$  latitude). Setting  $l = 0$ , perhaps roughly appropriate for the central Pacific Ocean, the two roots of Eq. (19) correspond, at a period of 2 weeks, to wavelengths of about 2500 and 50,000 km. The longer of these is so great that it would act dynamically as a nearly uniform elevation, generating almost no flow response. Visually, one might anticipate seeing only a single propagating wave with a wavelength of several thousand kilometers (as in the central Pacific Ocean).

If one now supposes that in the Southern Ocean, the comparatively narrow passages southward of Australia and South Africa force the solution to generate waves with a meridional length scale of  $l \approx 1 \times 10^{-6}$  ( $= 2\pi/6000$  km), then the two roots of Eq. (19) correspond to waves of

wavelengths of about 3200 and 8300 km—which are comparable and expected to generate a visually much more complex pattern not unlike what we see in the Southern Ocean.

This simple argument is, of course, too primitive to be more than suggestive. Barotropic Rossby waves interact strongly with topography, so that comparatively modest slopes,  $h_x/h$ ,  $h_y/h$ , generate “effective”  $\beta$ -values whose magnitudes  $|f(h_x/h, h_y/h)|$  can easily overwhelm the planetary value. Furthermore, the phase velocity of the flat-bottom modes is so small (about 3 cm/s for the 3200-km wave), that neglect of the mean flow in the model is likely to produce unrealistic results. Accurate long-period tide models will eventually require the presence of the oceanic general circulation.

## 11. ACKNOWLEDGEMENTS

Supported in part by the Jet Propulsion Laboratory under Contract 958125 at MIT and Rutgers. Development of the spectral element ocean model was supported at Rutgers by the Office of Naval Research under Contract N00014-93-0197. A.J. Miller, D. Cartwright and P. Woodworth made many useful suggestions. This paper was presented in honor of David Cartwright on his 70th birthday.

## 12. REFERENCES

- AGNEW D.C. and FARRELL W.E. (1978) Self-consistent equilibrium ocean tides. *Geophysical Journal of the Royal Astronomical Society* **55**, 171–181.
- BARNIER B. (1988) Numerical study on the influence of the mid-Atlantic ridge on nonlinear first-mode baroclinic Rossby Waves. *Journal of Physical Oceanography* **18**, 417–433.
- CARTON J.A. (1983) The variation with frequency of the long period tides. *Journal of Geophysical Research* **8**, 7563–7572.
- CARTON J.A. and WAHR J.M. (1986) Modelling the pole tide and its effect on the Earth’s rotation. *Geophysical Journal International* **84**, 121–137.
- CARTWRIGHT D.E. (1998) *Tides—A Scientific History*. Cambridge University Press, in press.
- CARTWRIGHT D.E. and EDDEN A.C. (1973) Corrected tables of tidal harmonics. *Geophysical Journal of the Royal Astronomical Society* **33**, 253–264.
- CARTWRIGHT D.E. and RAY R. (1990) Observations of the Mf ocean tide from GEOSAT altimetry. *Geophysical Research Letters* **17**, 619–622.
- CHENG M.K., EANES R.J. and TAPLEY B.D. (1992) Tidal deceleration of the Moon’s mean motion. *Geophysical Journal International* **108**, 401–409.
- CHRISTODOULIDIS D.C., SMITH D.E., WILLIAMSON R.G. and KLOSKO S.M. (1988) Observed tidal braking in the Earth/Moon/Sun system. *Journal of Geophysical Research* **93**, 6216–6236.
- DESAI S.D. and WAHR J.M. (1995) Empirical ocean tide models estimated from TOPEX/POSEIDON altimetry. *Journal of Geophysical Research* **100**(25), 205–225, 227.
- DICKMAN S.R. (1988) The self-consistent dynamic pole tide in non-global oceans. *Geophysical Journal of the Royal Astronomical Society* **94**, 157–174.
- DICKMAN S.R. (1989) A complete spherical harmonic approach to luni-solar tides. *Geophysical Journal International* **99**, 457–468.
- DOODSON A.T. (1921) The harmonic development of the tide-generating potential. *Proceedings of the Royal Society of London A* **100**, 305–329.
- GARRETT C. (1975) Tides in gulfs. *Deep-Sea Research* **22**, 23–36.
- GILL A.E. (1982) *Atmosphere–Ocean Dynamics*. Academic Press, New York.
- HAIDVOGEL D.B., CURCHITSER E., ISKANDARANI M., HUGHES R. and TAYLOR, M. (1997) Global modeling of the ocean and atmosphere using the spectral element method. In: *Atmosphere–Ocean*, XXXV, the Andre J. Robert Memorial Volume, C. LIN, R. LAPRISE and H. RITCHIE, editors, pp. 505–531. Canadian Meteorological and Oceanographic Society, Ottawa, Canada.

- HAUBRICH R. and MUNK W. (1959) The pole tide. *Journal of Geophysical Research* **64**, 2373–2388.
- HENDERSHOTT M.C. (1972) The effects of solid earth deformation on global ocean tides. *Geophysical Journal of the Royal Astronomical Society* **29**, 389–402.
- HENDERSHOTT M.C. (1981) Long waves and ocean tides. In: *Evolution of Physical Oceanography. Scientific Surveys in Honor of Henry Stommel*, B.A. WARREN and C. WUNSCH, editors, pp. 292–341. The MIT Press, Cambridge.
- ISKANDARANI M., HAIDVOGEL D.B. and BOYD J.P. (1995) A staggered spectral element model for the shallow water equations. *International Journal of Numerical Methods in Fluids* **20**, 393–414.
- JACKSON D.D. (1975) *Classical Electrodynamics*, 2nd ed. John Wiley, New York.
- KAGAN B.A., RIVKIND V.Y. and CHERNAYEV P.K. (1976) The fortnightly lunar tides in the world ocean. *Izvestiya, Atmospheric and Oceanic Physics* **12**, 449–452.
- LAMB H. (1932) *Hydrodynamics*, 6th ed. Dover, New York.
- LAMBECK K. (1980) *The Earth's Variable Rotation: Geophysical Causes and Consequences*. Cambridge University Press, Cambridge.
- LAMBECK K. (1988) *Geophysical Geodesy*. Oxford University Press, New York.
- LONGUET-HIGGINS M.S. (1968) The eigenfunctions of Laplace's tidal equations over a sphere. *Philosophical Transactions of the Royal Society of London A* **262**, 511–607.
- LONGUET-HIGGINS M.S. and POND G.S. (1970) The free oscillations of fluid on a hemisphere bounded by meridians of longitude. *Philosophical Transactions of the Royal Society of London A* **266**, 193–223.
- LUTHER D.S. (1980) Observations of long-period waves in the tropical oceans and atmosphere. Ph.D. dissertation, MIT and WHOI.
- LYARD C. and LE PROVOST C. (1997) Energy budget of the tidal hydrodynamic model FES94.1. *Geophysical Research Letters* **24**, 687–690.
- MARSH J.G. *et al.* (1990) The GEM-T2 gravitational model. *Journal of Geophysical Research* **95**, 22043–22071.
- MILLER A.J., LUTHER D.S. and HENDERSHOTT M.C. (1993) The fortnightly and monthly tides: resonant Rossby waves or nearly equilibrium gravity waves?. *Journal of Physical Oceanography* **23**, 879–897.
- MILLER S. and WUNSCH C. (1973) The pole tide. *Nature, Physical Science* **246**, 98–102.
- MORSE P.M. and FESHBACH H. (1953) *Methods of Theoretical Physics*, 2 vols. McGraw-Hill, New York.
- MUNK W.H. and MACDONALD G.J.F. (1960) *The Rotation of the Earth: A Geophysical Discussion*. Cambridge University Press, Cambridge.
- O'CONNOR W.P. (1995) The complex wavenumber eigenvalues of Laplace's tidal equation for oceans bounded by meridians. *Proceedings of the Royal Society of London, A* **449**, 51–64; Corrigendum, 1996, *Proceedings of the Royal Society of London, A* **452**, 1185–1187.
- PLATZMAN G.W., CURTIS G.A., HANSEN K.S. and SLATER R.D. (1981) Normal modes of the world ocean. Part II: Description of modes in the period range 8 to 80 hours. *Journal of Physical Oceanography* **11**, 579–603.
- RAY R.D. and CARTWRIGHT D.E. (1994) Satellite altimeter observation of the Mf and Mm ocean tides, with simultaneous orbit corrections. *Geophysical Monograph*, 82, *IUGG Monograph* **17**, 69–78.
- SCHUREMAN P. (1958) *Manual of Harmonic Analysis and Prediction of Tides*. US Department of Commerce, Special Publication No. 98.
- SCHWIDERSKI E.W. (1982) Global ocean tides, part X: the fortnightly lunar tide (Mf), atlas of tidal charts and maps. Report of the Naval Surface Weapons Center, TR-81-218, Dahlgren Va.
- SEILER U. (1990) Variations of the angular momentum budget for tides of the present ocean. In: *Earth's Rotation from Eons to Days*, P. BROSCHE and J. SÜNDERMANN, editors, pp. 81–94. Springer-Verlag, Berlin.
- TAYLOR G.I. (1919) Tidal friction in the Irish Sea. *Philosophical Transactions of the Royal Society of London A* **220**, 1–33.
- TRUPIN A. and WAHR J. (1990) Spectroscopic analysis of global tide gauge sea level data. *Geophysical Journal International* **100**, 441–453.
- TSIMPLIS M.N., FLATHER R.A. and VASSIE J.M. (1994) The North Sea pole tide described through a tide-surge numerical model. *Geophysical Research Letters* **21**, 449–452.
- WUNSCH C. (1967) The long-period tides. *Reviews of Geophysics* **5**, 447–476.
- WUNSCH C. (1986) Dynamics of the North Sea pole tide revisited. *Geophysical Journal of the Royal Astronomical Society* **87**, 869–884.
- XIE L. and DICKMAN S.R. (1996) Tide gauge analysis of the pole tide in the North Sea. *Geophysical Journal International* **126**, 863–870.